JOURNAL OF ENDOUROLOGY
Volume 25, Number 3, March 2011

Pp. 511–517
DOI: 10.1089/end.2010.0249

Kidney Deformation and Intraprocedural Registration: A Study of Elements of Image-Guided Kidney Surgery

Hernan O. Altamar, M.D.,[1] Rowena E. Ong,[2] Courtenay L. Glisson,[2] Davis P. Viprakasit, M.D.,[3] Michael I. Miga, Ph.D.,[2] Stanley Duke Herrell, M.D., FACS,[3] and Robert L. Galloway, Ph.D.[2]

Abstract

Introduction: Central to any image-guided surgical procedure is the alignment of image and physical coordinate spaces, or registration. We explored the task of registration in the kidney through *in vivo* and *ex vivo* porcine animal models and a human study of minimally invasive kidney surgery.

Methods: A set of ($n = 6$) *ex vivo* porcine kidney models was utilized to study the effect of perfusion and loss of turgor caused by incision. Computed tomography (CT) and laser range scanner localizations of the porcine kidneys were performed before and after renal vessel clamping and after capsular incision. The da Vinci™ robotic surgery system was used for kidney surface acquisition and registration during robot-assisted laparoscopic partial nephrectomy. The surgeon acquired the physical surface data points with a tracked robotic instrument. These data points were aligned to preoperative CT for surface-based registrations. In addition, two biomechanical elastic computer models (isotropic and anisotropic) were constructed to simulate deformations in one of the kidneys to assess predictive capabilities.

Results: The mean displacement at the surface fiducials (glass beads) in six porcine kidneys was 4.4 ± 2.1 mm (range 3.4–6.7 mm), with a maximum displacement range of 6.1 to 11.2 mm. Surface-based registrations using the da Vinci robotic instrument in robot-assisted laparoscopic partial nephrectomy yielded mean and standard deviation closest point distances of 1.4 and 1.1 mm. With respect to computer model predictive capability, the target registration error was on average 6.7 mm without using the model and 3.2 mm with using the model. The maximum target error reduced from 11.4 to 6.2 mm. The anisotropic biomechanical model yielded better performance but was not statistically better.

Conclusions: An initial point-based alignment followed by an iterative closest point registration is a feasible method of registering preoperative image (CT) space to intraoperative physical (robot) space. Although rigid registration provides utility for image-guidance, local deformations in regions of resection may be more significant. Computer models may be useful for prediction of such deformations, but more investigation is needed to establish the necessity of such compensation.

Introduction

GUIDANCE AND NAVIGATION during surgical procedures of the kidney traditionally depend on direct vision whether via open or laparoscopic approach. Image-guided surgery (IGS) attempts to reach beyond this limitation to surface anatomy and allow observation of subsurface objects by incorporating preoperative imaging to the intraoperative physical environment. By providing the surgeon a navigational aid, an image-guided kidney surgery system would allow the surgeon to optimize nephron-sparing oncologic resections and avoid unintended damage or intrusion to critical structures, such as blood vessels and the collecting system. The process of integrating the preoperative information with the real-time intraoperative physical environment requires a registration, defined as the alignment of multiple data sets and physical space into a single coordinate system such that the spatial locations of the corresponding points coincide.[1] In minimally invasive surgery of the kidney, the obstacles to an accurate and robust kidney localization and registration include a limited laparoscopic view, lack of adequate localization instrumentation, organ shift, and tissue deformation.

IGS and soft tissue navigation requires tracking devices or systems to execute the image to patient registration.[2]

[1]Department of Surgery, Uniformed Services University of the Health Sciences, Bethesda, Maryland.
[2]Department of Biomedical Engineering, Vanderbilt University, Nashville, Tennessee.
[3]Department of Urologic Surgery, Vanderbilt University Medical Center, Nashville, Tennessee.

FIG. 1. Container and tracked scalpel for porcine kidney incision. Left: scalpel with Polaris target attached to handle, used to track an incision made to the renal parenchyma. Right: porcine kidney with glass bead fiducials attached to the surface to track deformation. The kidney was perfused with saline and cut with tracked scalpel.

Minimally invasive surgery of the kidney introduces several challenges to this step. In laparoscopic and robotic surgery, access is provided through a series of small incisions. This limits the surface available for registration between localizer space and image space. The appropriateness of the da Vinci™ robot surgical system as part of an IGS system has been evaluated, and the accuracy of the device as a localizer in the operative setting has been previously demonstrated.[3–6] On the basis of this work, we also aimed to explore the use of the da Vinci surgical system for surface-based registrations during robot-assisted laparoscopic partial nephrectomy (RALPN).

Ideally, an image-guided kidney surgery system would not only account for changes in kidney position and orientation by performing a rigid alignment but also for changes in kidney shape that occur during surgery. For example, surgical conditions that may cause nonrigid kidney deformation are the loss of perfusion from clamping of the renal vessels as well as the loss of kidney turgor during partial nephrectomy. The extent of the deformation caused by intrarenal pressure decrease and whether it can be corrected for in an image-guided kidney surgery system are not well known. In this work, we attempt to measure and model beyond simple registration, the deformation that occurs when a kidney is subject to a parenchymal incision under a controlled renal arterial pressure.

Methods

Animal kidney protocol

An institutional animal care and use committee (IACUC)-approved porcine kidney animal protocol was utilized to assess the kidney deformation that occurs when the renal vessels are clamped and a parenchymal incision is made. Three pigs were heparinized and euthanized, and six kidneys were resected. Fifteen to twenty 2-mm glass bead fiducials, or physical reference points, were sutured to the kidney surface, and the kidney was fixed to an enclosing container to eliminate any rigid motion. The resected porcine kidneys were perfused with saline at renal arterial pressure of 100 mm Hg via cannulated artery and vein. Once protocol perfusion pressure was obtained, the renal artery and vein were clamped. Predeformation computed tomography (CT) of each

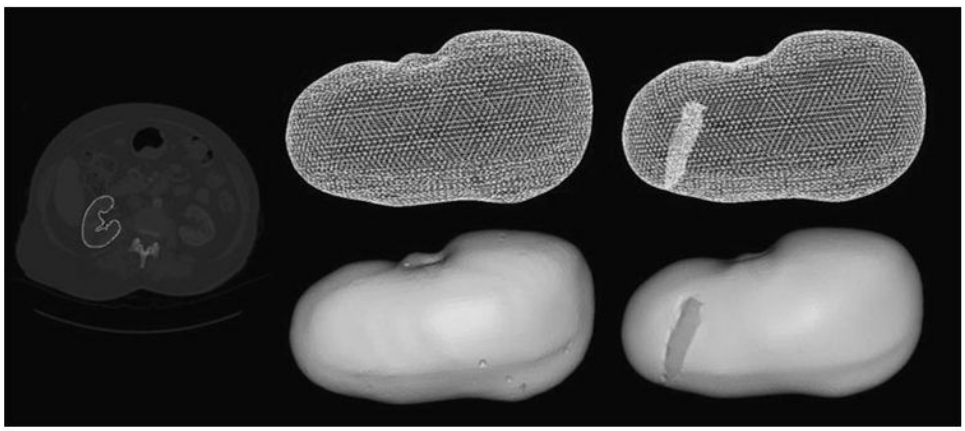

FIG. 2. Segmented computed tomography (CT) slice (left), three-dimensional kidney mesh (middle), and three-dimensional kidney mesh split along tracked incision (right).

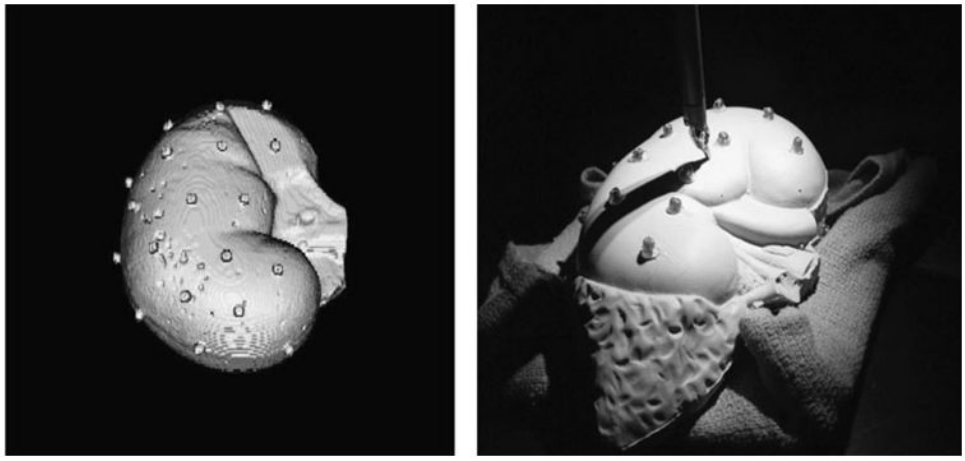

FIG. 3. Surface-based registration in kidney phantoms using a tracked robotic stylus. Left: volume rendering of CT volume of the kidney phantom with attached fiducial markers. Right: anthropomorphic kidney phantom with adrenal gland. The da Vinci robot with large needle driver was used to swab the surface of the kidney phantom. The cylindrical fiducial markers are also shown.

kidney was performed (90 keV, 300 mAs, 0.8 mm slice thickness). A scalpel whose tip was tracked using the Polaris Spectra (Northern Digital Inc., Ontario, Canada) infrared tracking device was used to make an incision in the renal parenchyma (Fig. 1). Six external fiducials glued to the kidney container were localized using the Polaris Spectra and the scalpel probe to register to preoperative kidney image (CT) space. Finally, a postdeformation CT image of the kidney was performed to assess the resulting deformation. To measure the amount of deformation, the glass fiducials were localized in the pre- and postdeformation images by calculating the intensity-based centroids. The mean shift at the surface fiducials was then calculated for the six kidneys.

Mathematical modeling and validation

An elastic model (Appendix 1) was chosen to describe the kidney deformation caused by incision and loss in turgor. Two models were constructed in which one model reflected isotropic mechanical properties, whereas the second reflected anisotropic mechanical properties to reflect the pyramidal structure of the renal tubules. The CT image volumes were segmented, three-dimensional finite element meshes were generated, the mesh was split to simulate the tracked incision, and the model was used to predict deformation for the third pig kidney (Fig. 2). The target registration error (TRE) was calculated as the average distance between the true displaced fiducial locations (found in the postdeformation image) and those predicted by the model. The magnitude error was calculated as the root mean square difference between the magnitudes of the true displacement vectors and those predicted by the model.

Robot-assisted laparoscopic partial nephrectomy

Surface-based kidney registrations were performed through an institutional review board (IRB)-approved protocol for RALPN. In previous work[3–6] the da Vinci robotic surgery system, via the patient side manipulators (surgical arms), was utilized to perform a surface-based method of registration between image space and physical space. The robotic arms and a tracked instrument, or stylus, served as the means of localizing the surgical target into the operative environment. It was demonstrated that the stylus tip can be tracked with a high level of accuracy.[4,5] This established robotic IGS (RIGS) system has previously been applied to both tissue-mimicking silicone kidney phantoms (Ecoflex; Smooth-On Inc., Easton, PA) and, in this study, to the surgically dissected kidneys in human RALPN. Herrell et al[6] evaluated the use of the RIGS for a surface-based method for registration. The process was validated utilizing anthropomorphic kidney phantoms with radiologically visible fiducial markers on the surface as follows: four anatomic points were touched and recorded, at each the upper pole, lower pole, lateral margin, and hilum; an iterative closest point algorithm was used to allow the RIGS-obtained surface data set and the preoperative image set to settle together; and the quality of the registration was determined by examining the distance between the

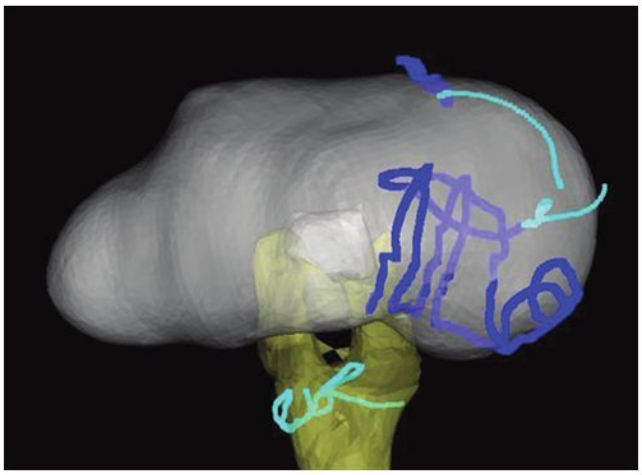

FIG. 4. The dark blue lines were used for registration with image from CT. Cyan areas of the kidney and on the hilum were not used to create transformation matrix. Registration was applied to held-out kidney and hilum data.

Table 1. Amount of Deformation That Occurred When Six Pig Kidneys Were Perfused at 100 mm Hg, Clamped, and Then Cut with a Scalpel

	Displacement at surface fiducials (mm)		
Kidney	*Mean*	*Standard deviation*	*Max*
1	4.7	2.2	9.2
2	3.4	2.0	7.4
3	6.7	2.4	11.4
4	4.5	2.2	7.2
5	3.8	1.7	6.1
6	3.4	1.8	5.7
Mean	4.4	2.1	

Displacement was tracked using glass fiducials, localized from pre- and postdeformation computed tomography images, and the mean shift at these surface fiducials was then calculated.

surfaces and the registration error of the fiducial (target) points (Fig. 3).

After informed consent, kidney surface data points were acquired intraoperatively on patients with renal masses undergoing RALPN. Surgical dissection of the renal hilum and unveiling of the kidney surface was performed as routine for the planned RALPN. A da Vinci tool, the large needle driver, was moved across the surface of the kidney undergoing resection. The surgeon kept the tip of the tool, as best possible, just resting on the surface. The location of the tool was recorded as previously described,[5] a sparse surface was created, and this robotically obtained surface was registered to the preoperative CT surface using an iterative closest point algorithm. In Figure 4 the dark blue points were used for the surface registration and the cyan points were held out of the registration. When the transformation was created, that transformation was applied to the cyan points to see where they would land. In addition, points on or near the vascular insertions into the hilum were marked.

Results

The amount of deformation that occurred when six porcine kidneys were perfused at 100 mm Hg, clamped, and then incised with a scalpel is shown in Table 1. The mean deformation for all six kidneys was 4.4 mm. The magnitudes of the displacements as distributed across the surface of the kidney

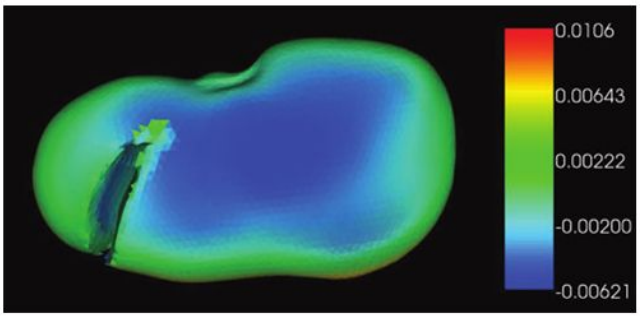

FIG. 6. Mesh deformed by anisotropic linear elastic model, where color represents the signed distance between the predeformation and model-deformed meshes for kidney 3. Negative distances represent where model-deformed mesh has sunken in and positive distances where the mesh has expanded out.

can be seen in Figure 5. Here we observed that the displacement magnitudes in general decrease with increased distance from the incision.

Model validation

The general pattern of deformation predicted by the anisotropic linear elastic model is shown in Figure 6, which displays the signed closest distance between the pre- and postdeformation meshes. Here we see that the model predicts a general "sinking in" of the kidney surface in the direction of gravity (indicated by the blue areas) and a small expansion along the lateral edges (indicated by the green areas). Figure 7 displays the model-predicted and true displacement vectors. The TRE and magnitude error for two simulations are shown in Table 2. The anisotropic linear elastic model performed better than the purely isotropic model. Although not statistically significant, this finding is consistent with the anatomical structure of the kidney.

Surface-based kidney registration

In utilizing the tracked robotic instrument to perform a surface-based registration, our results thus far are limited and lack a true measure of accuracy, the TRE. However, the results of this registration are qualitatively very good. The mean closest point distance was found to be 1.4 mm. We held out the points represented in cyan and only used the dark blue points

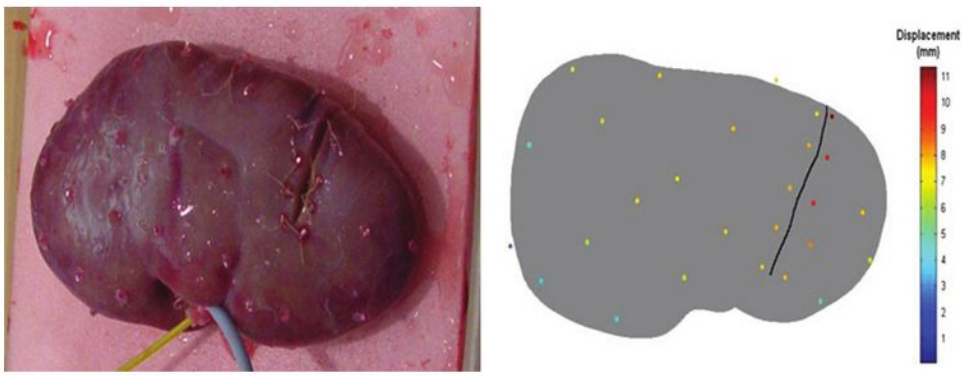

FIG. 5. Left: photograph of pig kidney 6 postincision. Fiducials attached to the surface can be seen. Right: fiducial locations color-coded by absolute distance change.

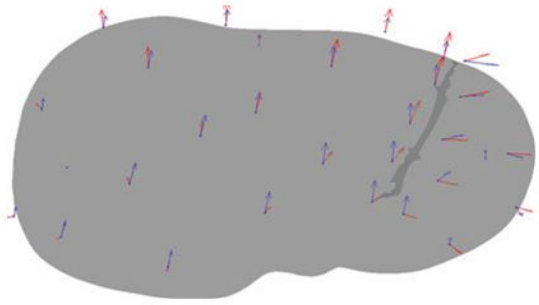

FIG. 7. Predeformation mesh for kidney 3 with blue arrows representing true displacements and red arrows representing displacements predicted by the anisotropic linear elastic model.

for the registration (Fig. 4). We then used the transformation obtained from the dark blue points and applied it to the cyan points that include the vascular locations beyond the hilum. Those points qualitatively aligned with the intended target.

Discussion

IGS[7] is well established in neurosurgery for the brain[8]; in ear, nose, throat surgery for sinus and skull base; and in orthopedics for spine surgery[9] and hip[10] and knee[11] replacement, where the tissue or surgical target exists in a relatively fixed position and pose intraoperatively and in the transfer from the preoperative to operative environment. In these surgical interventions point-based registrations can be performed on fixed external targets or fiducials.[12,13] For the urologist, particularly the minimal invasive surgeon, the relative location of internal organs compared with external structures is often dynamic depending on patient position, respiration, or other physiological and surgical processes.[14] This relative motion and restricted access make point-based registration methods less than ideal. Therefore, another method often used for IGS is surface-based registration methods.

Surface-based image registration methods use the shape of the organ surface to allow registration between the localizer and image space. Surface acquisition can be accomplished by many different methods, though commonly is accomplished using a laser range scanner. The optical line of sight tracking by laser range scanner yields a dense point cloud of surface anatomy and features. This equipment and type of registration have been incorporated into IGS systems for open procedures and are in use for hepatic surgery.[15–17] However, no such laparoscopic localization or tracking device exists. As such, the da Vinci surgical system and its incorporation into a RIGS system were previously explored.[3–5] Benincasa et al[18] demonstrated that the limited view of the kidney, to include veiling in perirenal fat, can be addressed through surface-based registration. They concluded that robust and accurate registrations were feasible when only 28% of the kidney surface area was exposed, and even less if regions of high curvature or anatomic distinction were included. This experience along with the use of the robot as a localizer led to our study. We found that as in the RIGS work on kidney phantoms our swabbing the human kidney with a tracked stylus yielded a good fit between the preoperative CT and the intraoperative physical kidney. This study, in combination with prior work, suggests that surface-based registration utilizing the da Vinci surgical system may provide acceptable intraprocedural registrations for IGS.

Table 2. Target Registration Error and Magnitude Error for Linear Elastic and Anisotropic Linear Elastic Models for Kidney 3

	TRE (mm)			*Magnitude error (mm)*		
	Mean	*Median*	*Max*	*Mean*	*Median*	*Max*
Linear elastic model	3.4	3.3	6.5	1.6	1.6	5.3
Anisotropic linear elastic	3.2	3.0	6.2	1.6	1.2	4.9

TRE, target registration error.

Organ shift and tissue deformation impose additional sources of error to the preoperative image to intraoperative physical space transformation. These factors inherent to soft tissue navigation and to image-guided kidney surgery support the development of intraprocedural registration methods and also highlight the importance of tissue deformation studies. The application of soft tissue modeling methods is a tool toward addressing these issues in surgical navigation. Fluid elastic models, a type of biomechanical model, provide some sophistication by allowing for different elasticity factors for varying regions of an organ. Previous work on kidney deformation modeling by Ong et al[19] demonstrated that the average amount of nonrigid kidney shift caused by loss of kidney perfusion was ~3 mm. When observing the deformation results from Table 1 for kidney 3 and the remaining TRE in Table 2, some understanding for the potential of computer models to compensate for nonrigid deformation can be obtained. In Table 1, the average fiducial deformation is 6.7 mm. In Table 2, the TRE becomes 3.2 mm on average after the use of the model. This suggests that the computer model in this study could compensate for ~52% of the deformation associated with the incision. Given the preliminary state of this work, this is very encouraging and awaits further study. Further, although the experiment performed was on *ex vivo* porcine kidneys that were free of lesions, these results may provide an estimate of the kidney shift that a human, tumor-containing, *in vivo* kidney may experience. In addition, this current study improves upon those preliminary results by controlling for the initial renal arterial pressure and accounting for parenchymal incisions.

The average amount of displacement for six pig kidneys was found to be between 3 and 6 mm. Analysis of displacement vectors at the fiducials shows that the absolute location changes primarily in one direction, that is, downward in the direction of gravity as the kidney loses turgor. This effect seems to be primarily caused by the loss of fluid and pressure within the kidney. Analysis of the fiducial locations on either side of the incision line is also useful. The fiducials on either side of the incision show the incision opening as you would suspect. From the origin of the incision to its termination for kidney 3, relative spacing of fiducials spanning the incision goes from 0.7 to 3.3 mm to 5.9 to 8.1 mm. So, the incision opening widens from the origin to the point of termination. Finally, the displacements seem to decrease in magnitude as the distance from the incision increases. One hypothesis that could explain this pattern is that the displacement magnitudes

could be proportional to amount of drainage in that area. Therefore, it would make sense that greater displacements might be seen in the areas closer to the incision than farther away, as there might be more drainage in that area. Compensating for these elements of kidney shift and deformation as tumor resection in the kidney proceeds would provide for real-time adjustments in an image-guided kidney surgery system.

Conclusions

With regard to intraprocedural registration, surface-based registration via a tracked robotic instrument is a small advance into the clinical arena from prior system validation in the laboratory setting. Through a nonrigid kidney deformation mathematical model, we were able to predict the tissue response to loss of perfusion and surgical incision in an *ex vivo* porcine kidney model. The preliminary model results show that about 50% of the kidney shift can be corrected for using such a model. Future work includes improving the model and exploring methods to address the extensive computational challenges associated with incorporating a model-based correction into an IGS system.

Disclosure Statement

Laboratory/animal study was funded in part by an educational grant from Pathfinder Therapeutics, Inc.

References

1. Fitzpatrick JM, Hill DLG, Maurer CR. Handbook of Medical Imaging, Volume 2. Medical Image Processing and Analysis. Bellingham, WA: SPIE Press, 2000.
2. Baumhauer M, Feuerstein M, Meinzer HP, Rassweiler J. Navigation in endoscopic soft tissue surgery: Perspectives and limitations. J Endourol 2008;22:751–766.
3. Kwartowitz DM, Miga MI, Herrell SD, Galloway RL. Towards image guided robotic surgery: Multi-arm tracking through hybrid localization. Int J Comput Assist Radiol Surg 2009;4:281–286.
4. Kwartowitz DM, Herrell SD, Galloway RL. Update: Toward image-guided robotic surgery: Determining the intrinsic accuracy of the da Vinci-S robot. Int J Comput Assist Radiol Surg 2007;1:301–304.
5. Kwartowitz DM, Herrell SD, Galloway RL. Toward image-guided robotic surgery: Determining intrinsic accuracy of the da Vinci robot. Int J Comput Assist Radiol Surg 2006; 1:157–165.
6. Herrell SD, Kwartowitz DM, Milhoua PM, Galloway, RL. Toward image guided robotic surgery: System validation. J Urol 2009;181:783–789.
7. Galloway RL. The process and development of image-guided procedures. Annu Rev Biomed Eng 2001;3:83–108.
8. Hall WA. The safety and efficacy of stereotactic biopsy for intracranial lesions. Cancer 1998;82:1749–1755.
9. Merloz P, Tonetti J, Eid A, et al. Computer assisted spine surgery. Clin Orthop Relat Res 1997;(337):86–96.
10. Bargar WL, Bauer A, Borner M. Primary and revision total hip replacement using the Robodoc system. Clin Orthop Relat Res 1998;(354):82–91.
11. Delp SL, Stulberg SD, Davies B, Picard F, Leitner F. Computer assisted knee replacement. Clin Orthop Relat Res 1998;(354):49–56.
12. Fitzpatrick JM, West JB, Maurer CR. Predicting error in rigid-body point-based registration. IEEE Trans Med Imaging 1998;17:694–702.
13. Fitzpatrick JM, West JB. The distribution of target registration error in rigid-body point-based registration. IEEE Trans Med Imaging 2001;20:917–927.
14. Teber D, Baumhauer M, Guven EO, Rassweiler J. Robotic and imaging in urological surgery. Curr Opin Urol 2009;19: 108–113.
15. Stefansic JD, Bass WA, Hartmann SL, et al. Design and implementation of a PC-based image-guided surgical system. Comput Methods Programs Biomed 2002;69:211–224.
16. Herline AJ, Herring JL, Stefansic JD, et al. Surface registration for use in interactive, image-guided liver surgery. Comput Aided Surg 2000;5:11–17.
17. Cash DM, Sinha TK, Chapman WC, et al. Incorporation of a laser range scanner into image-guided liver surgery: Surface acquisition, registration, and tracking. Med Phys 2003;30: 1671–1682.
18. Benincasa AB, Clements LW, Herrell SD, Galloway RL. Feasibility study for image-guided kidney surgery: Assessment of required intraoperative surface for accurate physical to image space registrations. Med Phys 2008;35:4251–4261.
19. Ong RE, Herrell SD, Miga MI, Galloway, RL. A kidney deformation model for use in non-rigid registration during image-guided surgery. Proceedings of the SPIE Medical Imaging: Visualization, Image-Guided Procedures, and Modeling 2008;6918.

Address correspondence to:
Hernan O. Altamar, M.D.
Department of Surgery
Uniformed Services University of the Health Sciences
Bethesda, MD 20814

E-mail: hernan.altamar@usuhs.mil

Abbreviations Used

CT = computed tomography
IGS = image-guided surgery
RALPN = robot-assisted laparoscopic partial nephrectomy
RIGS = robotic image-guided surgery
TRE = target registration error

(*Appendix follows* →)

Appendix 1. Mathematical Model

$$\nabla \cdot \sigma = 0,$$

where σ is the mechanical stress tensor. The boundary conditions for the model were set as follows: the bottom surface and hilum area of the kidney were fixed, a type 2 surface pressure of 70 Pa in the outward normal direction was applied at the incision, and a type 2 surface pressure of 1000 Pa was applied in the direction of gravity to simulate the loss of turgor caused by loss of intrarenal pressure. Two constitutive models were chose for study: (1) isotropic, and (2) planarly isotropic whereby cross-pyramidal track loading was considered isotropic and differing than loading along the pyramidal tracks. The model parameters for both models were as follows:

with Young's modulus as E, shear modulus as G, Poisson's ratio as ν, and the subscripts L and T representing properties along and transverse to the pyramidal structures of the renal tubules, respectively. The directions of the renal tubules were approximated by establishing a fixed-length medial axis of the kidney and allowing tubule directions to radiate out from the axis. For model properties, values used were estimated from the literature. Both models were solved using the Galerkin finite element method.

Material properties			
Isotropic		*Anisotropic*	
E	8000 Pa	E_L	10,000 Pa
ν	0.45	E_T	5000 Pa
		ν_{LT}	0.4
		ν_T	0.2
		G_{LT}	2083.33 Pa